ASYMPTOTIC ANALYSIS AND DESIGN OF LDPC CODES FOR LAURENT-BASED OPTIMAL AND SUBOPTIMAL CPM RECEIVERS

Tarik Benaddi †⋆‡ *Charly Poulliat* ⋆‡ *Marie-Laure Boucheret*⋆‡ *Benjamin Gadat* * *Guy Lesthievent* †

† CNES ⋆ University of Toulouse, ENSEEIHT/IRIT ‡ TéSA * Thales Alenia Space
E-mail: { Tarik.Benaddi, Charly.Poulliat, Marie-Laure.Boucheret } @enseeiht.fr
Benjamin.Gadat@thalesaleniaspace.com, Guy.Lesthievent@cnes.fr

ABSTRACT

In this paper, we derive an asymptotic analysis for a capacity approaching design of serially concatenated turbo schemes with low density parity check (LDPC) codes and continuous phase modulation (CPM) based on Laurent decomposition. The proposed design is based on extrinsic mutual information evolution and Gaussian approximation. By inserting partial interleavers between LDPC and CPM and allowing degree-1 variable nodes under a certain constraint we show that designed rates are very close to the maximum achievable rates. Furthermore, we discuss the selection of low complexity receivers that works with the same optimized profiles.

Index Terms— CPM, LDPC, EXIT Chart, code design, low complexity receiver, Laurent decomposition, iterative decoding

1. INTRODUCTION

Continuous phase modulations (CPM) represents a subset of phase modulation family where the phase is kept continuous between signal intervals. The phase continuity and the constant envelope characteristics allow CPM systems to achieve better spectral efficiency and bit error rates particularly when the system or the channel induces nonlinearities. Because of its interesting theoretical properties, this kind of modulation is considered with a cyclic interest as a good choice for different stringent communication systems.

After the advent of turbo-codes [1], coded CPM systems have greatly benefited from the concept of Turbo-processing. If several papers consider the serial concatenation of CPM with trellis based codes [2–5], only few references studied the concatenation with Low-Density Parity-Check (LDPC) codes. In most of cases, the proposed approaches are dedicated to specific family of CPM modulations and thus lack generality. The first related work is due to [6,7] where a study of the concatenated LDPC code + Minimum Shift Keying (MSK) has been performed using density evolution. It is shown that the optimal design depends on the implementation of the continuous phase encoder: if implemented as a recursive encoder, there is a design enabling interleaving gain, otherwise a non-iterative scheme with an optimal code for the binary case is sufficient. In [8], the author have studied Bit Interleaved Coded-Modulation approach to optimize M-ary CPFSK modulations. It allows to consider the design of the modulation and the external code separately. Finally, [9–11] have considered an irregular-repeat-accumulate (IRA) like concatenated scheme. The proposed structure replaces the IRA accumulator with a CPM modulator. This has been motivated by the fact that CPM can be seen as a phase accumulator. Furthermore, unlike the studied detectors in [12], Extrinsic Information Transfer (EXIT) curves of CPMs always join the point $(1, 1)$. This allows us to consider degree-1 variable nodes, which improve the achievable designed code rate as long as a certain stability condition is satisfied [13].

All these concatenated systems consider a full interleaving between the CPM and the outer code and a CPM trellis based on Rimoldi decomposition [14]. The corresponding optimal detector requires a filter bank whose size increases exponentially with the memory of the CPM. One common method to implement low complexity receivers is to use amplitude modulated pulses (AMP) decomposition [15]. Low complexity receivers can be designed, with a negligible performance degradation, using only the most significant components, remaining ones can be neglected or considered as interference [16, 17]. Surprisingly, no works have been conducted to study joint optimization of an LDPC code concatenated with such optimal or low complexity CPM demodulators. In [18], the authors have applied a curve fitting approach to design LDPC codes for GMSK considering a classical full interleaving between the LDPC code and the CPM. Actually, it leads to a nonlinear optimization approach. In this paper, we show that if a proper partial interleaver is used between the CPM and the LDPC code, the optimization can be linear. Moreover, it will be shown that introduction of degree-1 variable nodes is mandatory to design rates very close to the maximum achievable rates.

In this paper, we investigate bit-interleaved serially concatenated CPM with an LDPC outer code using iterative decoding. In this context, we derive an asymptotic optimization method. We point out that our optimization and its built-in scheduling can be applied to any other trellis-based coded modulation. It is also shown that performance of the generated LDPC codes remains optimal with low complexity receivers if a proper set of the Laurent components is selected. The paper is organized as follows. In Section 2, we give the system description, main notations and assumptions. The asymptotic analysis and the code design are given in Section 3. Simulation results are given in Section 4 and conclusions are drawn in Section 5.

2. SYSTEM DESCRIPTION

In this paper, we consider a serially concatenated coded scheme where a binary LDPC encoder is concatenated with a CPM modulator. At the transmitter, a binary message vector $\boldsymbol{u} \in GF(2)^K$ is first encoded using an LDPC code of rate $R = K/N$ to produce a codeword $\boldsymbol{c} \in GF(2)^N$. K is the number of information bits, N the codeword length and $GF(2)$ is the binary Galois field. An LDPC code is usually defined using its corresponding binary sparse parity check matrix H of size $M \times N$ with $M = N - K$. $\boldsymbol{c}$ is a binary vector that belongs to the null space of H, ie. $H\boldsymbol{c}^\top = \mathbf{0}$ where $^\top$ is the transposition operator. Based on H, an LDPC code can be rep-

978-1-4799-2893-4/14/$31.00 ©2014 IEEE

resented by its corresponding Tanner graph [19] as illustrated in Fig. 1. The Tanner graph consists in two sets of nodes: the variable nodes (circular vertices) associated with the codeword bits (columns of H) and the check node (black square vertices) associated with the parity check constraints (rows of H). An edge joins a variable node n to a check node m if $H(m,n) = 1$. Irregular LDPC codes are usually defined with their edge-perspective degree distribution polynomials $\lambda(x) = \sum_{i=1}^{d_v} \lambda_i x^{i-1}$ and $\rho(x) = \sum_{j=2}^{d_c} \rho_j x^{j-1}$ where λ_i (resp. ρ_j) is the proportion of edges in the Tanner graph connected to variable nodes (VN) of degree i (resp. to check nodes (CN) of degree j) and d_v (reps. d_c) is maximum VN (resp. CN) degree. When H is full rank, the design rate is given by $R = 1 - \sum_{j=2}^{d_c} \frac{\rho_j}{j} / \sum_{i=1}^{d_v} \frac{\lambda_i}{i}$.

The codeword $\boldsymbol{c}$ is then interleaved as shown in Fig. 1 using partial interleavers. It implies a random interleaving of LDPC codewords bits using a different interleaving patterns among variable nodes of the same degree. This is in contrast with previously mentioned approaches that mainly consider full interleaving between the LDPC code and the CPM as classically done for serially concatenated schemes. The rationale behind this assumption will be made clearer when presenting the asymptotic analysis. Each code word $\boldsymbol{c}$, after being interleaved, is mapped into $\boldsymbol{\alpha} = \{\alpha_i\}_i \in \{-1,+1\}^N$ using classical antipodal mapping $\{'0' \leftrightarrow +1, '1' \leftrightarrow -1\}$. Finally, $\boldsymbol{\alpha}$ is encoded by the binary CPM modulator. A binary CPM signal can be expressed as:

$$s(t,\boldsymbol{\alpha}) = \sqrt{\frac{2E_s}{T}} \cos\left(2\pi f_0 t + \theta(t,\boldsymbol{\alpha}) + \theta_0\right) = \Re[s_b(t,\boldsymbol{\alpha}) e^{j2\pi f_0 t}] \tag{1}$$

where

$$\theta(t,\boldsymbol{\alpha}) = \pi h \sum_{i=0}^{N-1} \alpha_i q(t - iT) \quad \text{with} \quad q(t) = \begin{cases} \int_0^t g(\tau)d\tau, t \le L \\ 1/2 \quad , \quad t > L \end{cases}$$

where f_0 is the carrier frequency, θ_0 the initial phase shift, $\theta(t,\boldsymbol{\alpha})$ the information carrying phase, $g(t)$ the frequency pulse, $h = 2k/p$ the modulation index, L the memory and $\Re$ the real part. Practically, the shape of $q(t)$ (rectangular (REC), raised-cosine (RC), Gaussian...) and the length L determine the smoothness of the signal.

Based on Laurent representation [15], the baseband signal in (1) can be written as the sum of $K = 2^{L-1}$ amplitude modulated pules (AMP) scaled with symbols $a_{k,n} = e^{j\pi h A_{k,n}}$ as follows:

$$s_b(t) = \sqrt{2E_s/T} \sum_{k=0}^{K-1} \sum_{n=0}^{N-1} e^{j\pi h A_{k,n}} c_k(t - nT) \tag{2}$$

$$c_k(t) = s_0(t) \prod_{j=1}^{L-1} s_{j+L\beta_{k,j}}(t), \quad 0 < k < K-1$$

$$A_{k,n} = \sum_{i=0}^{n} \alpha_i - \sum_{j=1}^{L-1} \alpha_{n-j}\beta_{k,j} \quad , \quad s_j(t) = \frac{\sin(\psi(t+jT))}{\sin(\pi h)}$$

$$\psi(t) = \begin{cases} 2\pi h q(t) \quad 0 < t < LT \\ \pi h - 2\pi h q(t - LT) \quad LT < t < 2LT \\ 0 \quad \text{elsewhere} \end{cases}$$

where $\beta_{k,j}$ is the j^{th} bit in the radix-2 decomposition of the sum index k [15]. The baseband signal to be processed by the receiver can then be written as:

$$y(t) = s_b(t) + n(t), \quad t \in [LT, NT] \tag{3}$$

where $n(t)$ is an additive white Gaussian noise (AWGN), having a double-sided power spectral density N_0.

At the receiver, a classical serial iterative detection/demodulation and decoding procedure is performed using iteratively soft-input soft-output (SISO) detection/decoding modules for both CPM and LDPC decoders. LDPC decoding is performed using the suboptimal iterative belief propagation (BP) algorithm [19] based on log likelihood ratios (LLR). For the CPM, a SISO maximum a posteriori (MAP) receiver is derived. This is achieved by using the BCJR algorithm [20] on the corresponding CPM trellis. In the context of a Maximum Likelihood receiver, [16] first introduced the trellis corresponding to the Laurent's decomposition to apply Viterbi algorithm. At each trellis stage corresponding to the sampling period nT, all possible $a_{k,n}$ are given by the input symbol α_n and the phase state vector $X_n = [a_{o,n-L}, \alpha_{n-L+1}, ..., \alpha_{n-1}]$. Based on the same trellis, [17] then proposed to derive a MAP receiver using a filter bank adapted to $\{c_k(t)\}$. Applying the BCJR algorithm, the probability of the transition (X_{n-1}=x', X_n=x) can be factored as: $p(x', x, y(t)) = \alpha_{n-1}(x')\gamma_n(x', x)\beta_n(x)$, where $\alpha_{n-1}(x')$ and $\beta_n(x)$ are computed respectively with forward and backward recursions. [17] assumes that, under an AWGN assumption, the branch metric $\gamma_n(x', x)$ is proportional to the inner product $\Re\left(\sum_{k=0}^{K-1} y_{k,n} a_{k,n}^*\right)$ where $\{y_{k,n} = \int y(t) c_k^*(t - nT)dt\}$ are the outputs of matched filters $\{c_k^*(-t)\}$ sampled each nT.

Actually, for partial response CPM ($L > 1$), Laurent decomposition needs a whitening filter to decorrelate noise filtered by the matched filters $\{c_k^*(-t)\}$. Additionally, AMP whose support is greater than LT introduces inherently inter-symbol interference (ISI). For simplification reasons, we assume in this paper, as stated in [16, 17], that the effect of the ISI terms and the noise correlation can be neglected as the noise level is higher enough. In practice, we consider a log-MAP implementation of the BCJR algorithm computing extrinsic LLRs to feed the LDPC BP decoder.

Low complexity receivers can be derived by approximating the CPM signal with only $K' < K$ components. The new state vector is then written as $X'_n = [a_{0,n-L+i}, \alpha_{n-1}, ..., \alpha_{n-L+1+i}]$ where i depends on K' and $\beta_{k,j}$ in (2). Usually, we need only $K' \in \{1, 2\}$ instead of $K = 2^{L-1}$ to represent the perfect signal with good accuracy (Cf. Table 1, Figs. 2(a) and 2(b) for GSM GMSK (L=3, BT=0.3, g(t)=Gaussian) and 3MSK(L=3, g(t)=REC)).

CPM	1^{st} component	2^{nd} component	Others
3MSK	93%	6.25%	0.23%
3GMSK	99.6%	0.37%	2.6 10^{-4}%

Table 1: Examples of energy distribution in Laurent components

3. ASYMPTOTIC ANALYSIS AND CODE DESIGN

EXIT chart is an asymptotic tool used to analyze the convergence of concatenated iterative systems. It is shown in [12] that iterative decoding using BP or BCJR can be well approximated using a Gaussian approximation of exchanged LLRs. Thereby, we can evaluate messages by only tracking their variance σ^2. Input-output transfer functions of SISO components can then be computed. These functions represent the mutual information (MI) associated with extrinsic LLR messages at the output of SISO component versus the MI associated with the a priori LLR messages. For consistent Gaussian messages, we can give the associated MI using $J(\sigma)$ which is a monodimensional function of the variance of the LLR messages [21]:

$$J(\sigma) = 1 - E_x(log_2(1 + e^{-x})), x \sim N(\sigma^2/2, \sigma^2) \tag{4}$$

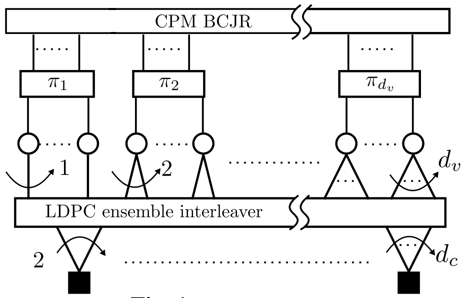

Fig. 1: Receiver model

In the following, to perform asymptotic analysis, we assume the following scheduling: a global iteration ℓ is composed of one BCJR iteration followed by one LDPC decoding iteration. We further assume partial interleavers associated with variables of degree i only. This assumption is in essence equivalent to [12], but it becomes crucial when using a trellis base detector. It is also implicitly assumed that BCJR recursions are independently run between different trellis section sets delimited by each VN-degree interleaver π_i (cf. Fig. 1). It is not the case in practice, but this assumption allows us to neglect transition effects when running the BCJR decoding pass.

Once the different EXIT charts have been obtained, we track the evolution of the mutual information of the messages exchanged in the BP decoding for a given signal-to-noise ratio (SNR). In this Section, we refer to the MI of the LLR values sent from component v to component w at the iteration ℓ as $I^{\ell}_{v,w}$. By abuse of notation, $I^{\ell}_{v,w}$ can refer to the extrinsic information between extrinsic LLR values of v and corresponding bits or to the prior MI between prior LLR values of w and their relative bits.

3.1. CPM EXIT transfer function and analysis

Let $I_{cpm,A}$ (resp. $I_{cpm,E}$) denotes the a priori (resp. the extrinsic) MI associated with a priori LLR messages at the input (resp. extrinsic LLR messages at the output) of the SISO CPM decoder. Then the input-output EXIT transfer characteristic (also referred to as EXIT curve) is formally given as:

$$I_{cpm,E} = T_{cpm}(I_{cpm,A}) \tag{5}$$

where $T_{cpm}(.)$ is the EXIT transfer function of the SISO CPM demodulator implicitly depending on the SNR. Analytic expressions of $T_{cpm}(.)$ are usually not available, but they can be evaluated by Monte Carlo simulations [21]. In practice, $T_{cpm}(.)$ is approximated by a polynomial curve fitting. As we will consider a curve fitting approach for the proposed code design and based on the commonly observed generalization of the results of [22] for the Binary Erasure Channel, an upper bound on the achievable rate for the outer serially concatenated LDPC code can be efficiently estimated using the area under the CPM detector EXIT curve, i.e.: $R \leq R^* = \int_0^1 T_{cpm}(I_{cpm,A})d(I_{cpm,A})$. Fig. 2 depicts the achievable rates R^* of GSM GMSK and 3MSK CPM configurations and their EXIT charts at E_s/N_0=-5,0,5dB. Moreover, for 3MSK, since $c_1(t)$ is not negligible compared to $c_0(t)$ (cf. Fig. 2(a)), considering only the first order approximate modifies considerably the EXIT charts (cf. Fig. 2(e)) and produces a loss of rate when R^*=0.5 of almost 0.5dB (cf. Fig. 2(c)). In this case, a second order approximate is needed. Whereas for GMSK, the first component $c_0(t)$ is sufficient (Fig. 2(b)) to remain a good approximation of the optimal detector EXIT (Fig. 2(f)). The idea behind considering enough AMP is that the same optimized LDPC code can be used with either optimal or reduced complexity CPM receivers.

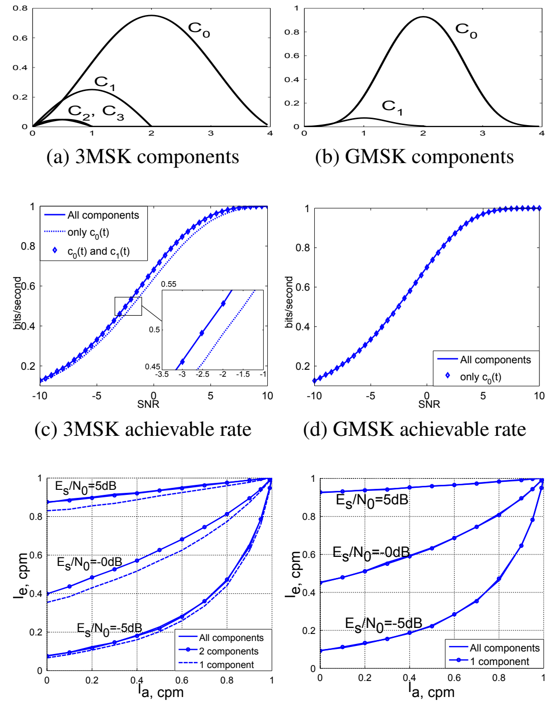

(a) 3MSK components (b) GMSK components

(c) 3MSK achievable rate (d) GMSK achievable rate

(e) 3MSK EXITS (f) GMSK EXITS

Fig. 2: Laurent components, R^* rate and EXIT for GMSK and 3MSK

3.2. Combined EXIT transfer function of VNs and CPM

Using the scheduling introduced at the beginning of the Section, we now derive a combined EXIT function for the VN and the SISO CPM module. For a degree-i VN, the extrinsic LLR $L_{m,out}$ on the m^{th} edge at the (global) iteration ℓ is computed as:

$$L^{\ell}_{m,out} = L^{\ell}_{cpm} + \sum_{k=1,k\neq m}^{i} L^{\ell-1}_{k,in}, \quad \forall m = 1...i$$

where L^{ℓ}_{cpm} is the extrinsic LLR from the SISO CPM decoder and $L^{\ell-1}_{k,in}$ are the LLRs from the adjacent check nodes from the previous iteration. Let $I^{\ell}_{vn,cn}(i)$ be the average MI associated with LLR messages passed from a VN of degree i to CNs at the ℓ^{th} iteration. Then, the average MI related to messages send from VNs to CNs is given as

$$I^{\ell}_{vn,cn} = \sum_{i=1}^{d_v} \lambda_i I^{\ell}_{vn,cn}(i) \tag{6}$$

Under Gaussian approximation [23], $I^{\ell}_{vn,cn}(i)$ is given by:

$$I^{\ell}_{vn,cn}(i) = J\left(\sqrt{(i-1)[J^{-1}(I^{\ell-1}_{cn,vn})]^2 + [J^{-1}(I^{\ell}_{cpm,vn}(i))]^2}\right)$$

where $I^{\ell}_{cpm,vn}(i)$ is the average MI for degree-i VN only associated with LLR messages from the CPM decoder to the LDPC decoder and $I^{\ell-1}_{cn,vn}$ the average MI associated with LLR messages from CN to VN. Due to the partial interleavers between the LDPC and the CPM and the assumption of independent BCJR decoding for VNs of different degrees, $I^{\ell}_{cpm,vn}(i)$ can be simply related to $I^{\ell-1}_{cn,vn}$ by

$$I^{\ell}_{cpm,vn}(i) = T_{cpm}(J(\sqrt{i}J^{-1}(I^{\ell-1}_{cn,vn}))) \tag{7}$$

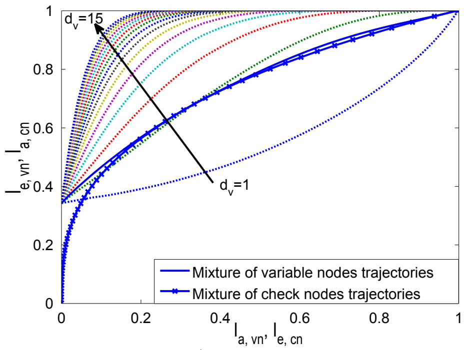

Fig. 3: VN and CN EXIT at $E_s/N_0 = -2dB$. Dashed lines refers to VN with different degrees.

Combining (7) and (6), one can draw the combined VN-CPM EXIT function. Fig. 3 plots different VN trajectories as function of node degrees. Observe that VNs EXITs do not start from the origin $(0, 0)$. The reason is that VNs observe the channel via CPM. Degree-1 VN EXIT corresponds actually to the EXIT transfer function of the SISO CPM decoder. We are then allowed to consider degree-1 VNs as in [6].

3.3. EXIT Transfer Function of CNs

For a degree-j check node, the extrinsic LLR $L^{\ell}_{m,in}$ on the m^{th} edge is computed using the so-called *tanh rule*:

$$\tanh\left(L^{\ell}_{m,in}/2\right) = \prod_{k=1,k\neq m}^{j} \tanh\left(L^{\ell}_{k,out}/2\right)$$

where $L^{\ell}_{k,out}$ are the a priori LLRs at the input of the CN. Using reciprocal channel approximation [12], which remains a good approximation for several channels, the average MI $I_{cn,vn}$ associated with extrinsic LLR messages passed from CN to VN at iteration $\ell-1$ is given by

$$I^{\ell-1}_{cn,vn} = 1 - \sum_{j=2}^{d_c} \rho_j J(\sqrt{j-1}J^{-1}(1 - I^{\ell-1}_{vn,cn})) \qquad (8)$$

where $I^{\ell-1}_{vn,cn}$ is the average MI associated with LLR messages from VNs to CNs.

3.4. Asymptotic Code design

Combining (5), (6), (7) and (8), we finally get:

$$I^{\ell}_{vn,cn} = F(\lambda(x), \rho(x), T_{cpm}(.), I^{(\ell-1)}_{vn,cn})$$

This recursion is a linear function with respect to parameters $\lambda_i, i = 1 \dots d_v$ for a given $\rho(x)$ and a given SNR. Assuming concentrated $\rho(x)$ [23], design rate maximization is equivalent to maximizing the cost function $\sum_i \lambda_i/i$ under to the constraints:

$$[C0] \text{ Mixture: } \quad \sum_i \lambda_i = 1$$

$$[C1] \text{ Convergence: } \quad F\left(\lambda(x), \rho(x), T_{cpm}(.), y\right) > y$$

$$[C2] \text{ Stability: } \quad \lambda_1 < 1/\left(\sum_{j=2}^{d_c} \rho_j (j-1) T'_{cpm}(1)\right) \qquad [13]$$

where $T'_{cpm}(.)$ is the derivative of T_{cpm}. This system can be efficiently solved by classical linear programming using discretization of the convergence constraint for $y \in$ [0,1].

GMSK all components				3MSK all components			
$R^* = 0.5063$ at $E_s/N_0 = -2.5$dB				$R^* = 0.5043$ at $E_s/N_0 = -2.4$dB			
$R = 0.5048$ at $E_s/N_0 = -2.4$dB				$R = 0.5033$ at $E_s/N_0 = -2.3$dB			
$d_{v,i}$	λ_i	$d_{c,i}$	ρ_i	$d_{v,i}$	λ_i	$d_{c,i}$	ρ_i
1	0.1294	4	0.25	1	0.1475	4	0.5
2	0.5148	5	0.75	2	0.5450	5	0.5
5	0.0679			5	0.0223		
10	0.2879			10	0.2852		

MSK			
$R^* = 0.5069$ at $E_s/N_0 = -2.5$dB			
$R = 0.4981$ at $E_s/N_0 = -2.5$dB			
$d_{v,i}$	λ_i	$d_{c,i}$	ρ_i
1	0.1273	4	0.3
2	0.5201	5	0.7
5	0.0577		
10	0.2949		

Table 2: Optimized LDPC codes for design rate $R = 0.5$

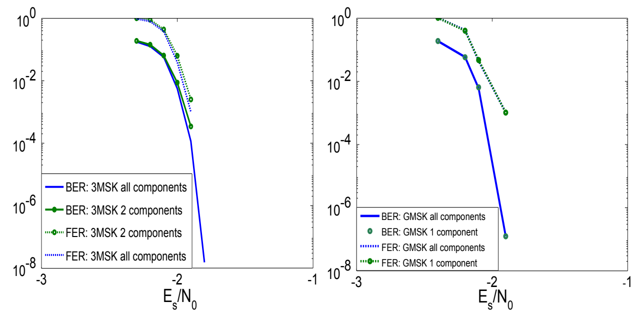

(a) 3MSK (b) GMSK

Fig. 4: BER and FER for optimized concatenated LDPC code with 3MSK and with GMSK

4. SIMULATION RESULTS

This section gives simulation results for binary LDPC code optimization for GSM GMSK and 3MSK, when $R^* = 0.5$. Simulations were performed using around 16000 information bits and 250 turbo iterations. Table 2 summarizes the optimized degree distributions for targeted design rates. We can observe that it is possible to operate at less than 0.1 dB from R^* for both GMSK and 3MSK when $d_v = 10$ only. Results can be improved with higher d_v.

Fig. 4 depicts 3MSK and GMSK Bit Error Rate (BER) and Frame Error Rate (FER) results. As expected in the analysis, we observe that for the same designed LDPC code, the optimal receiver of 3MSK outperforms the low complexity receiver designed with a suitable number of components by only 0.03dB for 10^{-4}. Same results can be drawn for GMSK. Considering less components would imply the design of specific profiles.

5. CONCLUSION

We introduced an asymptotic design of LDPC-CPM codes with respect to optimal and low complexity receivers. The proposed design can also handle the code rate adaptation since our approach allows to consider the design of the modulation and the external code separately. Nonetheless, computing capacities and rates with Gaussian approximation gives generally optimistic results. Future research will be dedicated to true density evolution analysis and related optimization. Using our approach, other interesting schemes can be considered using sparse graph-based codes such as IRA codes.

6. REFERENCES

[1] Claude Berrou and Alain Glavieux, "Near optimum error correcting coding and decoding: Turbo-codes," *IEEE Transactions on Communications*, vol. 44, no. 10, pp. 1261–1271, 1996.

[2] Par Moqvist and Tor M Aulin, "Serially concatenated continuous phase modulation with iterative decoding," *IEEE Transactions on Communications*, vol. 49, no. 11, pp. 1901–1915, 2001.

[3] Alexandre Graell i Amat, Charbel Abdel Nour, and Catherine Douillard, "Serially concatenated continuous phase modulation for satellite communications," *IEEE Transactions on Wireless Communications*, vol. 8, no. 6, pp. 3260–3269, 2009.

[4] Krishna R Narayanan and Gordon L Stuber, "A serial concatenation approach to iterative demodulation and decoding," *IEEE Transactions on Communications*, vol. 47, no. 7, pp. 956–961, 1999.

[5] R Chaggara, ML Boucheret, C Bazile, E Bouisson, A Ducasse, and JD Gayrard, "Continuous phase modulation for future satellite communication systems in ka band," in *Information and Communication Technologies: From Theory to Applications, 2004. International Conference on Proceedings. 2004*. IEEE, 2004, pp. 269–270.

[6] Krishna R Narayanan, Ibrahim Altunbas, and R Sekhar Narayanaswami, "Design of serial concatenated msk schemes based on density evolution," *IEEE Transactions on Communications*, vol. 51, no. 8, pp. 1283–1295, 2003.

[7] KR Narayanan, I Altunbas, and R Narayanaswami, "On the design of ldpc codes for msk," in *Global Telecommunications Conference, 2001. GLOBECOM'01. IEEE*. IEEE, 2001, vol. 2, pp. 1011–1015.

[8] Aravind Ganesan, *Capacity estimation and code design principles for continuous phase modulation (CPM)*, Ph.D. thesis, Texas A&M University, 2003.

[9] Ming Xiao and Tor Aulin, "Irregular repeat continuous phase modulation," *IEEE communications letters*, vol. 9, no. 8, pp. 723–725, 2005.

[10] Shi Cheng, Matthew C Valenti, and Don Torrieri, "Coherent continuous-phase frequency-shift keying: parameter optimization and code design," *IEEE Transactions on Wireless Communications*, vol. 8, no. 4, pp. 1792–1802, 2009.

[11] Ming Xiao and Tor M Aulin, "On analysis and design of low density generator matrix codes for continuous phase modulation," *IEEE Transactions on Wireless Communications*, vol. 6, no. 9, pp. 3440–3449, 2007.

[12] Stephan ten Brink, Gerhard Kramer, and Alexei Ashikhmin, "Design of low-density parity-check codes for modulation and detection," *IEEE Transactions on Communications*, vol. 52, no. 4, pp. 670–678, 2004.

[13] Thomas J Richardson, Mohammad Amin Shokrollahi, and Rüdiger L Urbanke, "Design of capacity-approaching irregular low-density parity-check codes," *IEEE Transactions on Information Theory*, vol. 47, no. 2, pp. 619–637, 2001.

[14] Bixio E Rimoldi, "A decomposition approach to cpm," *IEEE Transactions on Information Theory*, vol. 34, no. 2, pp. 260–270, 1988.

[15] P Laurent, "Exact and approximate construction of digital phase modulations by superposition of amplitude modulated pulses (amp)," *IEEE Transactions on Communications*, vol. 34, no. 2, pp. 150–160, 1986.

[16] Ghassan Kawas Kaleh, "Simple coherent receivers for partial response continuous phase modulation," *IEEE Journal on Selected Areas in Communications*, vol. 7, no. 9, pp. 1427–1436, 1989.

[17] Peter A Murphy, Gary E Ford, and Michael Golanbari, "Map symbol detection of cpm bursts," *Kluwer International Series in engineering and Computer Science*, pp. 199–210, 1997.

[18] Aimin Zhu, Xiaogang Huang, and Senjie Yao, "Design of optimal ldpc code for the system of gmsk concatenated with ldpc codes," in *2nd International Conference on Control, Instrumentation and Automation (ICCIA), 2011*. IEEE, 2011, pp. 168–171.

[19] R Tanner, "A recursive approach to low complexity codes," *IEEE Transactions on Information Theory*, vol. 27, no. 5, pp. 533–547, 1981.

[20] Lalit Bahl, John Cocke, Frederick Jelinek, and Josef Raviv, "Optimal decoding of linear codes for minimizing symbol error rate (corresp.)," *IEEE Transactions on Information Theory*, vol. 20, no. 2, pp. 284–287, 1974.

[21] Stephan Ten Brink, "Convergence behavior of iteratively decoded parallel concatenated codes," *IEEE Transactions on Communications*, vol. 49, no. 10, pp. 1727–1737, 2001.

[22] Alexei Ashikhmin, Gerhard Kramer, and Stephan ten Brink, "Extrinsic information transfer functions: model and erasure channel properties," *IEEE Transactions on Information Theory*, vol. 50, no. 11, pp. 2657–2673, 2004.

[23] Sae-Young Chung, Thomas J Richardson, and Rüdiger L Urbanke, "Analysis of sum-product decoding of low-density parity-check codes using a gaussian approximation," *IEEE Transactions on Information Theory*, vol. 47, no. 2, pp. 657–670, 2001.